Proc. 4th Int. Symp. on Smart Control of Turbulence
Tokyo, March 2-4, 2003

Suboptimal turbulence control algorithm for the modification of Reynolds stress in the near-wall layer

Koji Fukagata [1, 2] and Nobuhide Kasagi [1]
[1] *Department of Mechanical Engineering, The University of Tokyo*
7-3-1 Hongo, Bunkyo-ku, Tokyo 113-8656, Japan
[2] *Institute for Energy Utilization, AIST, 1-2-1 Namiki, Tsukuba-shi, Ibaraki 305-8564, Japan*
fukagata@thtlab.t.u-tokyo.ac.jp

We propose a new explicit control algorithm for drag reduction in wall-turbulence, which requires the streamwise wall-shear signal only. The cost function is designed to reduce the near-wall Reynolds shear stress that is responsible for the turbulent skin friction drag [K. Fukagata, K. Iwamoto, and N. Kasagi, Phys. Fluids **14**, L73 (2002)]. The solution to minimize the cost function is derived by using the suboptimal control technique applied to the Stokes equation [C. Lee, J. Kim, and H. Choi, J. Fluid Mech. **358**, 245 (1998)]. Numerical test shows over 10% drag reduction in turbulent pipe flow at $Re_\tau \simeq 180$.

1. Introduction

For a successful development of an active feedback control system for drag reduction in wall-bounded turbulent flow, the effectiveness of the control algorithm used, as well as the performance of the hardware components such as sensors and actuators, is of great importance.

Control algorithms may be classified into to types — *explicit* and *implicit* algorithms. What we call here the explicit algorithm is one in which the control input, ϕ, can be given explicitly, e.g, $\phi = F(s)$, where s is the sensor information and F is a mapping function. On the other hand, the implicit algorithm, such as the optimal control (e.g., Bewley et al., 2001), requires iterative procedures to determine the control input. While such implicit algorithms are useful to explore the possibility of drag reduction control, the explicit algorithms are more suited to real applications in which real-time computation is required.

In the last decade, various explicit control algorithm were developed and assessed by using direct numerical simulation (DNS) of controlled turbulent flow. Choi et al. (1994) proposed so-called the opposition control in that blowing/suction velocity is given at the wall so as to oppose the velocity components at a virtual detection plane located above the wall. They attained about 25 % drag reduction in their DNS of turbulent channel flow at low Reynolds numbers. Subsequently, several attempts were made to develop control algorithms using the information measurable at the wall. Lee et al. (1997) used a neural network and obtained an algorithm in which the control input is given as a weighted sum of the spanwise wall-shear stress, $\partial w/\partial y|_w$. Lee et al. (1998) derived series of analytical solution of the control input to minimize the cost function in the framework of the suboptimal control. Their DNS of channel flow at $Re_\tau \simeq 110$

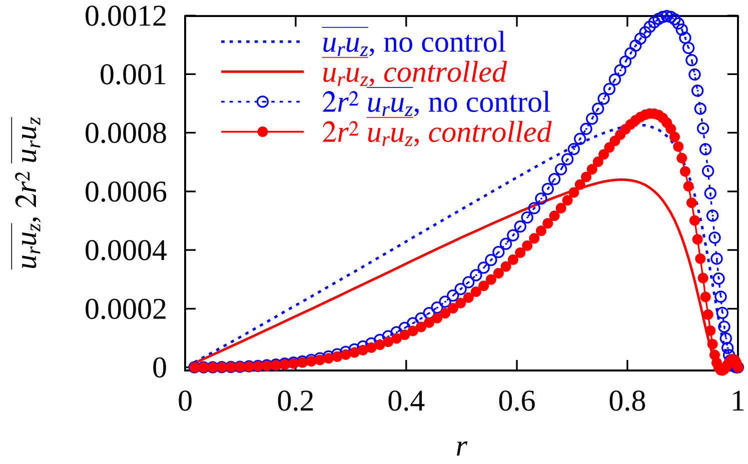

Figure 1: Raw and weighted Reynolds stress distribution (Fukagata et al., 2002).

showed 16-22% drag reduction when $\partial w/\partial y|_w$ (in this case, the control law is quite similar to that obtained by using the neural network mentioned above) or the wall pressure, p_w, was used as the sensor signal.

From the practical point of view, it is desirable to use the streamwise wall-shear stress, $\tau_w = \partial u/\partial y|_w$, or p_w (or both) as a sensor signal because a streamwise wall-shear stress sensor (Yoshino et al., 2003) and a wall pressure sensor (Löfdahl et al., 1996) of sufficiently small size and high frequency response are becoming available. For the use of p_w, in addition to the work by Lee et al. (1998), Koumoutsakos (1999) presented an algorithm to suppress the vorticity flux, and succeeded to reduce the friction drag in his DNS. For the use of τ_w, however, development of effective algorithm has remained unsuccessful. Actually, Lee et al. (1998) mentioned above also presented a suboptimal solution aiming at reduction of $\overline{\tau_w}$. This algorithm uses τ_w as the sensor signal only, but the friction drag (i.e., $\overline{\tau_w}$) was not reduced by that algorithm.

Very recently, Lee et al. (2001) applied a two-dimensional linear-quadratic-Gaussian (LQG) controller to a linearized Navier-Stokes equation. About 10 % drag reduction was attained in their DNS of a channel flow at $Re_\tau \simeq 100$. They also attained 17 % drag reduction by making an *ad hoc* extension. Morimoto et al. (2002) assumed the control input as a weighted sum of τ_w and optimized the weights by using the genetic algorithm (GA). The most excellent gene, i.e., the pattern of weights, led to 12 % drag reduction in a channel flow at $Re_\tau \simeq 100$. However, it is uncertain whether the two-dimensional controller or GA-optimized controller is the optimal one, because they depend on the prescribed assumptions. Therefore, in the present study, we attempt to analytically construct, without assumptions, an algorithm which uses τ_w only.

2. Theoretical background

Under the condition of constant flow rate, the skin friction drag, $C_f = \overline{\tau_w^*}/[(1/2)\rho^* U_b^{*2}]$, in fully developed channel and pipe flows can be decomposed as

$$C_f = \frac{12}{Re_b} + 12\int_0^1 2(1-y)(-\overline{u'v'})\,dy \qquad (1)$$

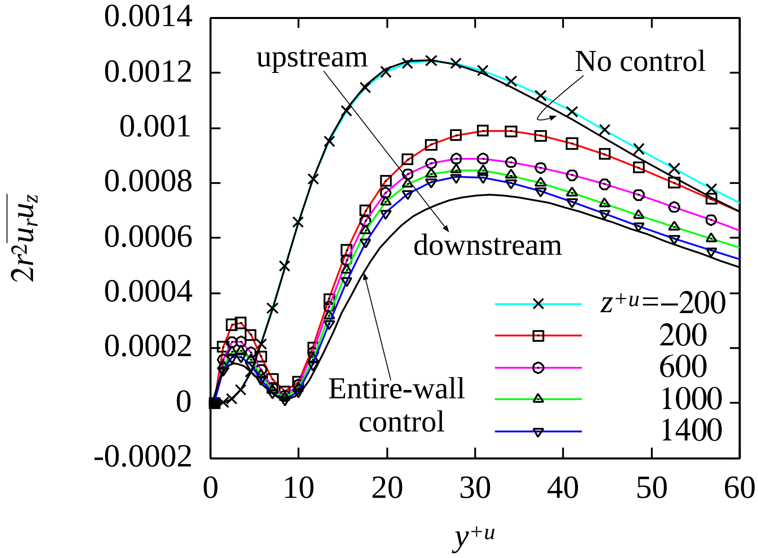

Figure 2: Variation of weighted Reynolds stress distribution downstream of the onset of control (Fukagata & Kasagi, 2003).

and

$$C_f = \frac{16}{Re_b} + 16 \int_0^1 2r\,\overline{u_r' u_z'}\,rdr\,, \tag{2}$$

respectively (Fukagata et al., 2002). Here, all variables without superscript are those nondimensionalized by the channel half width, δ^*, or the pipe radius, R^*, and twice the bulk mean velocity, $2U_b^*$, whereas dimensional variables are denoted by the superscript of $*$. The bulk Reynolds number is defined as

$$Re_b = \frac{2U_b^* \delta^*}{\nu^*}, \text{ or } Re_b = \frac{2U_b^* R^*}{\nu^*}\,, \tag{3}$$

Equations (1) and (2) indicates that the skin friction coefficient is decomposed into the laminar contribution that is identical to the well-known laminar solution, and a turbulent contribution which is proportional to the weighted integral of Reynolds shear stress. Figure 1 shows the Reynolds stress, $\overline{u_r' u_z'}$, and the weighted Reynolds stress appearing in Eq. (2) (i.e., $2r^2\overline{u_r' u_z'}$), in a pipe flow controlled by the opposition control algorithm (Fukagata et al., 2002). The difference in the areas covered by these two (controlled and uncontrolled) curves of the weighted Reynolds stress is directly proportional to the drag reduction by control. It is clear that most of the drag reduction is attributed to the suppression of near-wall Reynolds stress.

Another observation in Fig. 2 is that the Reynolds stress far from the wall is also suppressed, although what is directly suppressed due to the formation of a virtual wall (Hammond et al., 1998) should be the near-wall Reynolds stress only. This can be explained by a gradual propagation of the drastic change of near-wall Reynolds stress, which is similar to that observed in the pipe flow with the opposition control applied partially to wall (Fukagata & Kasagi, 2003), as illustrated in Fig. 2. At the beginning of controlled region ($z^{+u} = 200$), the profile near the wall ($y^{+u} < 40$) drastically changes due to the direct suppression. Then, the distribution far from the wall changes gradually following the quick change in the near-wall region. Although the control input in this example is turned on in space, a similar phenomena is expected when it

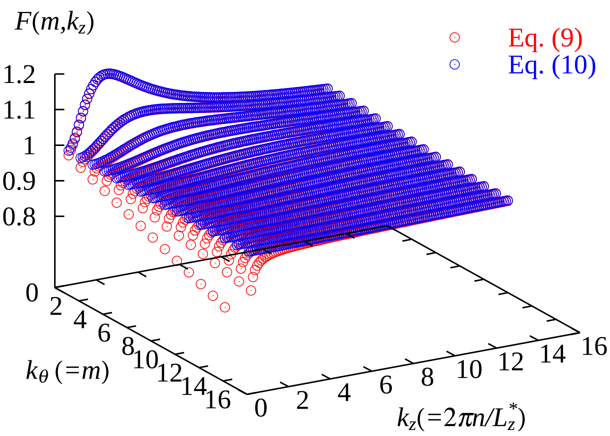

Figure 3: Correction factor, $F(m,\ k_z)$ $(C = 0.0013)$.

is turn on at a certain time to an fully developed uncontrolled flow.

3. Derivation of the control algorithm

The above-described knowledge suggests that suppression of the near-wall Reynolds shear stress is of primary importance in order to reduce the skin friction drag. Once the the near-wall Reynolds shear stress is suppressed, its propagation toward the direction far from the wall is also expected for an additional drag reduction. Therefore, we propose a cost functional $\mathcal{J}$ to be minimized as follows:

$$\mathcal{J}(\phi) = \frac{\ell}{2A\Delta t}\int_S\int_t^{t+\Delta t}\phi^2\,dt\,dS - \frac{1}{2A\Delta t}\int_S\int_t^{t+\Delta t}(-u'v')_{y=Y}\,dt\,dS\,. \tag{4}$$

Here, ϕ denotes the control input, i.e., the blowing/suction velocity at the wall, A is the area of wall, Δt is the time-span for optimization, and ℓ is the price for the control.

At first, a channel flow is considered for simplicity. The Reynolds shear-stress above the wall $(y = Y)$ is approximated by using the Taylor expansion as,

$$\left.\begin{aligned} u'(Y) &= Y\left.\frac{\partial u'}{\partial y}\right|_w + O(Y^2) \\ v'(Y) &= \phi + O(Y^2) \end{aligned}\right\} \Longrightarrow -u'v'(Y) = -Y\phi\left.\frac{\partial u'}{\partial y}\right|_w + O(Y^2)\,. \tag{5}$$

Substitution of Eq. (5) into Eq. (4) yields an approximated cost functional, i.e.,

$$\mathcal{J}(\phi) = \frac{\ell}{2A\Delta t}\int_S\int_t^{t+\Delta t}\phi^2\,dt\,dS - \frac{Y}{2A\Delta t}\int_S\int_t^{t+\Delta t}\phi\left.\frac{\partial u'}{\partial y}\right|_w\,dt\,dS\,. \tag{6}$$

The control input, ϕ, that minimize the cost functional, Eq. (6), can be calculated analytically by the procedure proposed by Lee et al. (1998). As the result, the suboptimal control input is obtained as

$$\widehat{\phi} = \frac{C}{1/\lambda - ik_x/k}\left.\frac{\widehat{\partial u}}{\partial y}\right|_w\,, \tag{7}$$

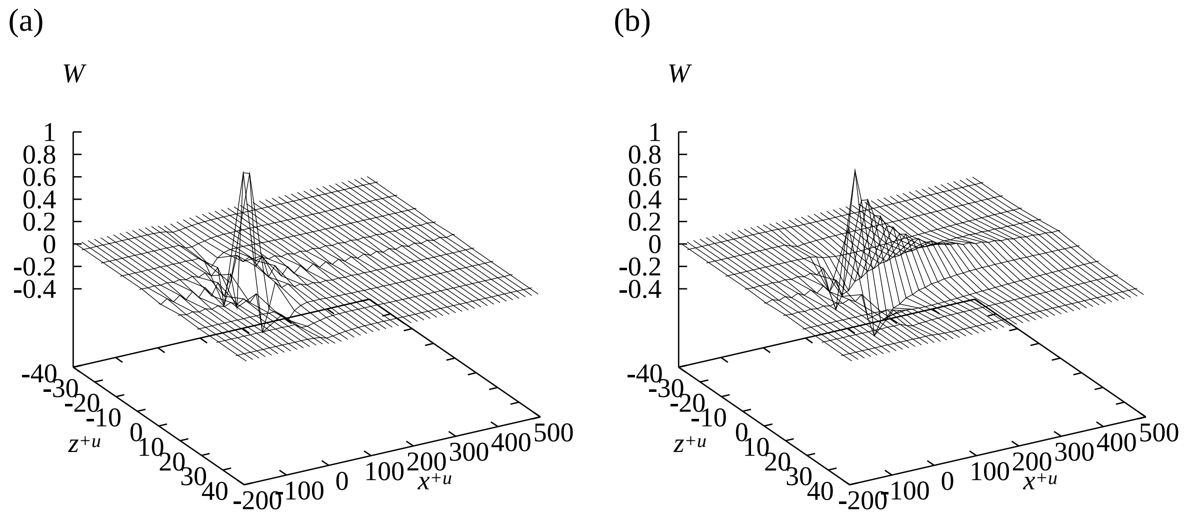

Figure 4: The normalized weights in the physical space: (a) $\lambda = 7$; (b) $\lambda = 73$.

where hat denotes the Fourier component and $k = \sqrt{k_x^2 + k_z^2}$. There are two parameters in this algorithm: $C = \sqrt{\Delta t / 2Re}$ is the amplitude coefficient and $\lambda = (Y/2\ell)\sqrt{2Re/\Delta t}$ can be interpreted as an informative downstream length as explained below.

A similar algorithm can be developed also for a pipe flow. Following the procedure by Xu et al. (2002), we obtain

$$\widehat{\phi} = \frac{C}{1/\lambda - iF(m,\, k_z)k_z/k} \left.\widehat{\frac{\partial u_z}{\partial r}}\right|_w , \tag{8}$$

where m is the azimuthal mode number and $k = \sqrt{k_z^2 + m^2}$. Here, the length is nondimensionalized by R^*, and hence $k_\theta = (2\pi m)/(2\pi R^*) = m$. The difference from the solution for channel flow is absorbed into the correction factor, $F(m,\, k_z)$, that is expressed, by properly approximating the modified Bessel function of higher orders, as

$$F(m, k_z) = \frac{k}{k_z}\left[\left(\frac{C}{2} + 1\right)\frac{I_m(k_z)}{I'_m(k_z)} - C\right] , \tag{9}$$

where $I_m(r)$ is the m-th order modified Bessel function, i.e., $I_m(r) = (-i)^m J_m(ir)$, and $I'_m(r)$ is its derivative. The amplitude parameter, C, is usually much smaller than unity. In that case, Eq. (9), can be simplified to read

$$F(m,\, k_z) = \frac{k}{k_z}\frac{I_m(k_z)}{I'_m(k_z)} . \tag{10}$$

The profile of $F(m\, k_z)$ in the case with typical value of C is drawn in Fig. (3). The correction factor is nearly unity for higher wave numbers. Naturally, the largest deviation is observed at the lowest azimuthal wavenumber ($m = 1$). Although the deviation is also observed at small k_z, large m modes, this may not much influence the control input because k_z/k is small.

The derived control algorithms can be transformed to the physical space through the following inverse Fourier transform:

$$\widehat{\phi} = \widehat{W}^* \left.\widehat{\frac{\partial u}{\partial y}}\right|_w \quad \Longrightarrow \quad \phi(x,z) = \int_{-\infty}^{\infty}\int_{-\infty}^{\infty} W(x',z') \left.\frac{\partial u}{\partial y}\right|_w (x+x', x+z')dx'dz' , \tag{11}$$

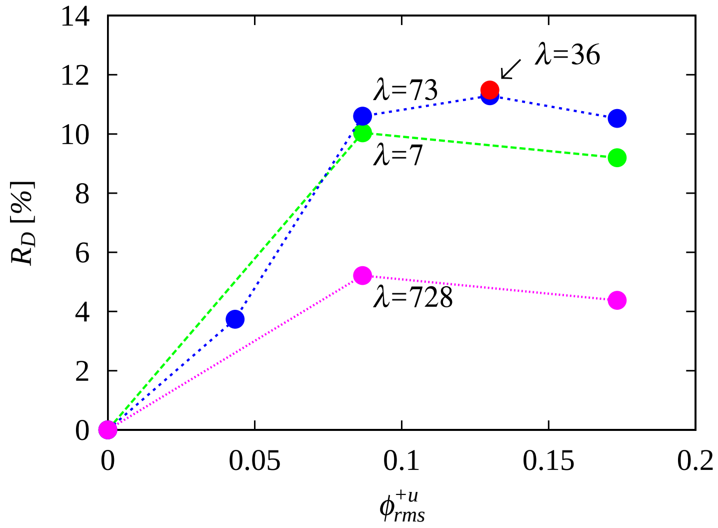

Figure 5: Drag reduction rate, R_D.

where $\widehat{W}^*$ is the function preceding τ_w in Eqs. (7) and (8). This indicates that the control input of an actuator is given by a weighted integration of τ_w around it. The weight, W, has two characteristics, as shown in Fig. 4 for the case of channel flow. One is something like a negative spanwise second derivative of τ_w. The other is the exponential decrease downstream of the actuator, of which length scale is determined by λ. The weight for the pipe flow is found to be essentially the same.

4. Performance test

Performance of the proposed control algorithm is tested by DNS of turbulent pipe flow. The DNS code is based on the energy conservative finite difference method for the cylindrical coordinate system. (Fukagata & Kasagi, 2002). The time integration is done by using the low storage third-order Runge-Kutta/Crank-Nicolson scheme (Spalart et al., 1991) The bulk mean velocity U_b is kept constant, and the Reynolds number is $Re_b = 5300$ ($Re_\tau = u_\tau^* R^{=ast}/\nu^* \simeq 180$ for uncontrolled flow). The computational domain has a longitudinal length of $L = 20R$ and the periodic boundary conditions are applied at both ends. The root mean square of the control input, ϕ_{rms}, is kept constant.

Figure 5 shows the computed drag reduction rate for different values of λ and ϕ_{rms}^{+u}. Here, the superscript of $+u$ denotes the wall unit of uncontrolled flow. For any values of λ tested here, large drag reduction rate is obtained when ϕ_{rms}^{+u} is of order of 0.1. This amplitude is nearly the same as that of the opposition control with the detection plane height of $y_d^{+u} \simeq 10$. The optimum value of λ seems to be between 10-100.

Figure 6 shows the Reynolds shear stress near the wall. As can be seen, with the present control the near-wall Reynolds stress is suppressed as intended. More interestingly, it takes negative values in $0 < y^{+u} < 5$ region. This suggests that drastic drag reduction may be attained even if the near-wall turbulent structure can be manipulated directly. All we have to do is to make a largely negative Reynolds stress in the near-wall layer. Development of the methodology to realize this is left for the future work.

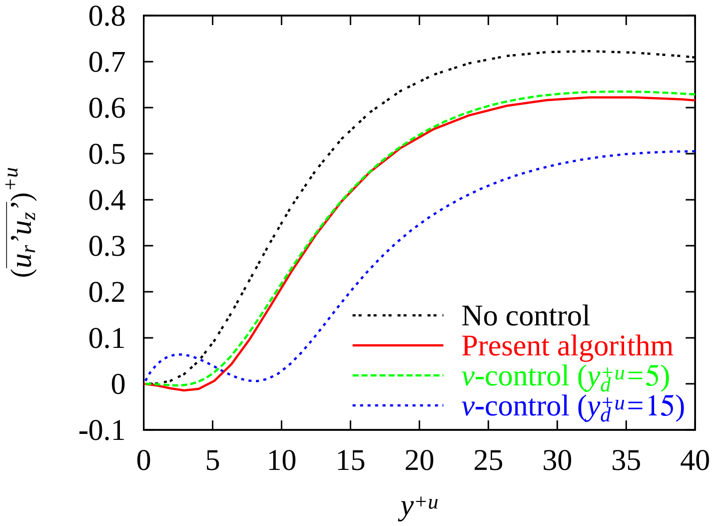

Figure 6: Reynolds stress ($\lambda = 73$, $\phi^{+u}_{rms} = 0.08$).

5. Conclusions

Based on the knowledge on the componential contribution to the skin friction (Fukagata et al, 2002), an alternative cost functional for drag reduction, which incorporate the near-wall Reynolds shear stress, was proposed in the framework of the suboptimal control. The control input to minimize that cost functional was analytically obtained by using the method proposed by Lee et al. (1998).

DNS of pipe flow at $Re_\tau \simeq 180$ with the proposed control algorithm showed 11-12% drag reduction, which is a comparable value to those obtained by using the two-dimensional LQG controller (Lee et al., 2001) and the GA-based algorithm (Morimoto et al., 2002). Although the drag reduction effect by the present algorithm was small, the results gave a hint toward further (and drastic) drag reduction by manipulation at the wall only.

References

Bewley, T.R., Moin, P., and Temam, R, 2001. DNS-based predictive control of turbulence: an optimal benchmark for feedback algorithms. *J. Fluid Mech.* **447**, 179-225.

Choi, H., Moin, P. and Kim, J., 1994. Active turbulence control for drag reduction in wall bounded flows. *J. Fluid Mech.* **262**, 75-110.

Fukagata, K., Iwamoto, K, and Kasagi, N., 2002. Contribution of Reynolds stress distribution to the skin friction in wall-bounded flows. *Phys. Fluids* **14**, L73-L76.

Fukagata, K. and Kasagi, N., 2002. Highly energy-conservative finite difference method for the cylindrical coordinate system. *J. Comput. Phys.* **181**, 478-498.

Fukagata, K. and Kasagi, N., 2003. Drag reduction in turbulent pipe flow with feedback control applied partially to wall. *Int. J. Heat Fluid Flow* **24**, (to appear).

Hammond, E.P., Bewley, T.R., Moin, P., 1998. Observed mechanisms for turbulence attenuation and enhancement in opposition-controlled wall-bounded flows. *Phys. Fluids* **10**, 2421-2423.

Koumoutsakos, P., 1999. Vorticity flux control for a turbulent channel flow. *Phys. Fluids* **11**, 248-250.

Lee, C., Kim, J., Babcock, D., and Goodman, 1997. Application of neural networks to turbulence control for drag reduction. *Phys. Fluids* **9**, 1740-1747.

Lee, C., Kim, J. and Choi, H., 1998. Suboptimal control of turbulent channel flow for drag reduction. *J.*

Fluid Mech. **358**, 245-258.

Lee., K.H., Cortelezzi, L., Kim, J., and Speyer, J, 2001. Application of reduced-order controller to turbulent flows for drag reduction. *Phys. Fluids* **13**, 1321-1330.

Löfdahl, L., Kälvesten, E., and Stemme, G, 1996. Small silicon pressure transducers for space-time correlation measurements in a flat plate boundary layer. *J. Fluids Eng.* **118**, 457-463.

Morimoto, K., Iwamoto, K., Suzuki, Y., and Kasagi, N, 2002. Genetic algorithm-based optimization of feedback control scheme for wall turbulence. In: *Proc. 3rd Int. Symp. on Smart Control of Turbulence, Tokyo, March 3-5, 2002*, pp. 107-113.

Spalart, P.R., Moser, R.D., Rogers, M.M., 1991. Spectral methods for the Navier-Stokes equations with one infinite and two periodic directions. *J. Comput. Phys.* **96**, 297-324.

Xu, C.-X., Choi, J.-I., Sung H.J., 2002. Suboptimal control for drag reduction in turbulent pipe flow. *Fluid Dyn. Res.* **30**, 217-231.

Yoshino, T., Suzuki, Y., Kasagi, N., and Kamiunten, S., 2003. Optimum design of micro thermal flow sensor and its evaluation in wall shear stress measurement, In: *Proc. IEEE Int. Conf. MEMS'03, Kyoto, Jan. 2003*, pp. 193-196.